Fast multielement phase-controlled photoacoustic imaging based on limited-field-filtered back-projection algorithm

Diwu Yang, Da Xing,[a] Huaimin Gu, Yi Tan, and Lvming Zeng
Institute of Laser Life Science, South China Normal University, Guangzhou 510631, China

(Received 28 March 2005; accepted 1 September 2005; published online 31 October 2005)

In this paper, the multielement phase-controlled technique and the limited-field -filtered back-projection algorithm are used to investigate the two-dimensional fast noninvasive photoacoustic imaging. By the use of the former to collect photoacoustic signals, which are of high signal-to-noise ratio, one needs not to average the data and can acquire them in less than 5 s. The later can greatly improve the lateral resolution of the multielement linear transducer array imaging system from 1.5 mm to 0.24 mm. This method and system can provide a fast and reliable approach to photoacoustic imaging that could be applied to noninvasive imaging and clinic diagnosis. © *2005 American Institute of Physics*. [DOI: 10.1063/1.2119417]

In photoacoustic (PA) imaging, laser pulses with a duration of several nanoseconds are used to heat absorbing structures within the tissue. The heated structures expand and become sources of acoustic waves, which can be detected by high sensitive piezoelectric devices outside the tissue. With photoacoustic signals generation, the strength and the profile of a photoacoustic signal depends on tissue optical absorption, which is often related to the physiological and pathological status of the tissue; thus the collected PA signals can be reconstructed to map the distribution of radiation absorption within the tissues. The sensitivity and resolution of PA imaging depend on the optical absorption contrast in tissues and ultrasound detection systems, such as the laser pulse duration, the geometry and the bandwidth of the ultrasound-detection system, and the image reconstruction algorithm, and so on.[1]

PA imaging combines the merits of both pure ultrasound imaging and pure optical imaging, and it can provide high ultrasonic resolution and high optical contrast tissue images. In recent years, PA image has become a popular research subject and suggested as new techniques for non-invasive imaging of blood vessels and tumors.[2–6] PA imaging of phantoms and *in vivo* functional imaging have been reported; many reconstruction algorithms are applied for the reconstruction of two-dimensional PA images.[7–12] In these experiments, the mechanical complication of experimental setup affects the reliability of the experimental measurement, and the long time for data acquisition and image reconstruction hampers the practical application of PA imaging. In our work, we have developed a multielement linear transducer array system (MLTAS) for PA imaging.[13,14] By using a phase-controlled technique to collect PA signals, the signal-to-noise ratio of the PA signals is high. The data need not be averaged, which can cut down much time required for data acquisition, and the total time of data acquisition is less than 5 s. Compared with single transducer collection, the PA imaging with MLTAS can eliminate the mechanical shift or rotation of the transducer. By taking advantage of these, we can effectively reduce the time and laser energy required for data acquisition, and can improve the reliability and convenience of PA imaging. A phase-controlled technique was used to detect time-trace signals, and the phase-controlled algorithm was used to reconstruct the image,[13] but the lateral resolution of the system obtained was not very well. Due to the directivity of the phase-controlled transducer array, there is a receiving solid angle along the acoustic axis of the array, within which photoacoustic signals can be collected. The receiving angle of a subarray of a 320-element linear transducer array is about 1.8° measured by experiment. In our previous work, we ignored the receiving angle and reconstructed the absorption distribution by directly back projecting the measured photoacoustic signals along the acoustic axis. Our latest experiments show that the resolution of the reconstructed image is intensively impacted by the receiving angle. In this paper, the limited-field-filtered back-projection algorithm is used for reconstructing the optical absorption distribution. The experimental results demonstrate that the limited-field filtered back projection algorithm can greatly improve the lateral resolution of the MLTAS; the lateral resolution of the system is improved from 1.5 mm to 0.24 mm.

The relationship between photoacoustic pressure and the distribution of optical absorption can be expressed as[7]

$$p(r,t) \approx -\frac{\beta I_0 \tau c_0}{4\pi c_p} \cdot \frac{d}{dt} \iint_{|r'-r_0|=c_0 t} A(r') \frac{dr'}{c_0 t}, \tag{1}$$

where $A(r')$ is the fractional energy-absorption per-unit-volume of soft tissue; β is the isobaric volume expansion coefficient; c_0 is the sound velocity in the target; c_p is the specific heat; $p(r,t)$ is the PA pressure; τ is the pulse width of pulse laser, respectively. Thus the PA pressure recorded at position r and time t is the sum of all pressure waves induced over the surfaces of a sphere of radius $|r'-r_0|$ in the tissue.

Because the subgroup of the linear transducer array has a characteristic impulse response, the photoacoustic pressure $p(r,t)$ at the detector position cannot be directly recorded. In practice, the measured signals $p'(r,t)$ are convolution of the PA pressure and the impulse response function $h(t)$, so we can compute $p(r,t)$ as

$$p'(r,t) = p(r,t)^* h(t). \tag{2}$$

Then $p(r,t)$ can be obtained by deconvoluting the impulse response of the transducer from the measured PA signal.

[a]Author to whom correspondence should be addressed; electronic mail: xingda@scnu.edu.cn

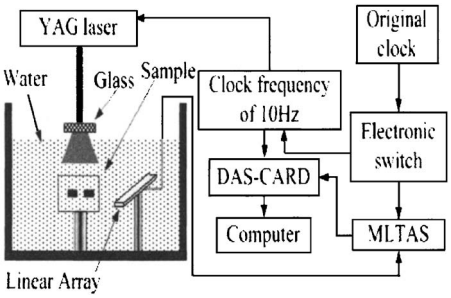

FIG. 1. Experimental setup for PA signals detection with MLTAS.

$$p(r,t) \approx IFFT\left[\frac{j\omega p'(\omega)}{I(\omega)}\right]\left[1+\cos\left(\frac{\pi\omega}{\omega_c}\right)\right], \tag{3}$$

where $p'(\omega)$ and $I(\omega)$ were the Fourier transform of the PA signal $p'(r,t)$ and $h(t)$, the impulse response of the detector, ω_c is the cut-off frequency, the apodizing function $1+\cos(\pi\omega/\omega_c)$ is the window function used to band-limit the signals to ω_c. In this case $\omega_c=10$ MHz.

In our present experiments, a new B-mode system (Model CTS-200, SIUI, China) was modified as our platform with 320 vertical transducer elements. The resonance frequency of the transducers is 7.5 MHz, and the scanning width is 50 mm. The transducers are divided into 80 subgroups; each subgroup consists of four transducers, which are selected with the control circuit. The signals from the transducers, after preamplification and phase adjustment, are acquired with the data-acquisition system card (compuscope 12100, Gage Applied Co., Montreal, Quebec, Canada). The card features a high-speed 12-bit analog-to-digital converter with a sampling rate of 100 MHz. The system operation and data collection are controlled by a personal computer.

The schematic of the experimental setup is shown in Fig. 1. A Q-switched ND: YAG laser operated at 1064 nm with pulse duration of 7 ns. A 20 Hz clock signal, provided by a control circuit, was used for triggering the laser and selecting the subgroup in the linear transducer array to capture PA signals, and triggering the data-acquisition system card. A piece of ground glass was used to homogenize the laser beam. The incident energy density was controlled below 20 mJ/cm^2. A EUZ-PL21 linear array was fixed and pointed to the center of the sample stage. The linear transducer array and phantom were both immersed in water for better coupling of acoustic waves.

In the first experiment, a cylindrical turbid phantom, which was made with 13% gelatin, 12.5% milk, and 74.5% water, was used to simulate the optical properties of human breast. The effective attenuation coefficient of the phantom is 1.2 cm^{-1}. The phantom contained two graphite rods with the same diameter, 0.7 mm, and the distance between them was 1.3 mm. The targets were embedded in the cylindrical phantom at a depth of 2 mm. In the second experiment, measurements were performed on blood vessels in the ear of a rabbit *in vivo*. The rabbit was anaesthetized. And the ear of the rabbit was shaved and placed on a mold. The ear of the rabbit was immerged in water to ensure a good acoustic coupling. An optical fiber (core diameter 600 μm, NA=0.22) was used to deliver light pulses to the samples from upside. The linear transducer array was placed pointed to the phantom to collect the PA signals. After 64 series of data were recorded, projections were calculated according to Eq. (3).

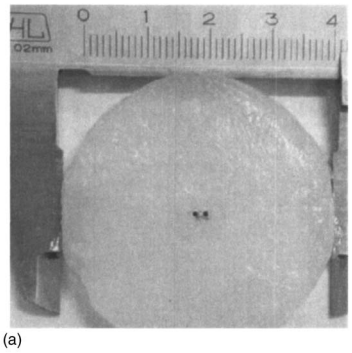

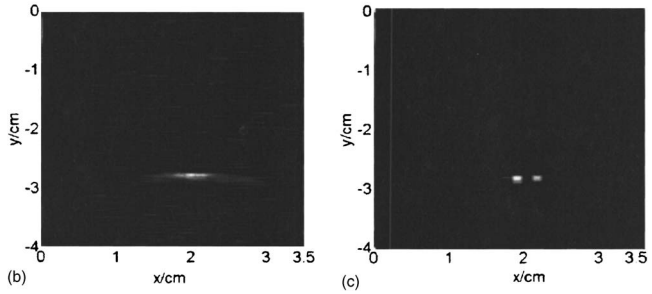

FIG. 2. Reconstructed image of the two-graphite-rods phantom. (a) The picture of phantom. (b) The reconstructed image with the phase-controlled algorithm. (c) The reconstructed image with the limited-field filtered back projection algorithm.

Images were reconstructed with the limited-field-filtered back-projection algorithm.

Figure 2(a) shows the physical dimensions of the test sample, Fig. 2(c) shows the reconstructed two-dimensional image with the limited-field-filtered back-projection algorithm applied in limited fields, and Fig. 2(b) shows the reconstructed image with phase-controlled algorithm, respectively. The reconstruction results clearly show that the contrast of the two images is very good. The reason is that using the phase-controlled technique to collect PA signals, the signal intensity for each position of the interest is the sum of the signals from the transducers at many positions, summing up signals from N different positions has a similar effect to signal averaging from N sampling, thus the signal-to-noise ratio is high. Figure 2(c) shows that the relative locations and sizes of the two-photoacoustic sources are clearly resolved and can perfectly match the original ones. But in Fig. 2(b) the two sources can no longer be clearly distinguished, and the sources have joined as a single object in the image. It demonstrates that the lateral resolution of reconstructed image in Fig. 2(c) is much better than that of the reconstructed image in Fig. 2(b). Because the collected signals by phase-controlled technique are not strictly from the acoustic axis of the array, but from a solid angle. So if the signals collected from the receiving solid angle are directly back projected along the acoustic axis of the array with the phased-controlled algorithm, the lateral segments of the reconstructed image would be broadened; and if the signals are back projected with the filtered back projection algorithm in the same limited fields within which the signals are collected, the reconstructed image can correctly match the absorption distribution, and can avoid lateral broadening.

To estimate the spatial resolution of the reconstructed images with the limited-field-filtered back-projection algorithm, a reconstructed profile at position $y=-27.5$ mm of the image in Fig. 2(c) is shown in Fig. 3. The profile includes

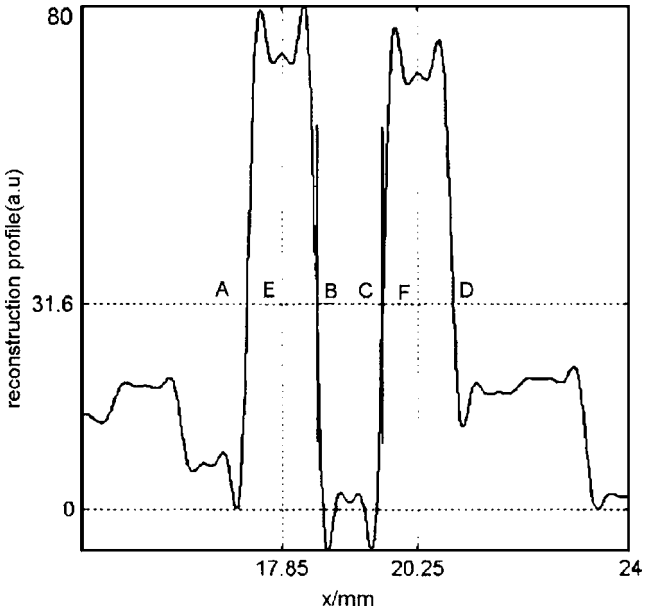

FIG. 3. The line profile of the reconstructed image shown in Fig. 2(c) with $y=-27.5$ mm.

two absorption sources. The 40.5%-amplitude line at $y=31.6$ intercepts with the profile at points A, B, C, and D. It also intercepts with the centerlines of the two absorption peaks at points E and F, respectively. The spatial resolution of the imaging system is estimated according to the Rayleigh criterion. Two sources can no longer be clearly distinguished when point B touches point C. Therefore, the minimum distinguishable distance, R, between two sources is approximately $R=|\mathrm{EB}|+|\mathrm{CF}|-2r$, where r is the radius of the absorption source. From Fig. 3, the minimum distance R, which is the spatial resolution of the imaging system, is determined as 0.24 mm.

Figure 4 shows the photoacoustic reconstruction of the parts of *in vivo* blood vessels in the ear of a rabbit by the limited-field-filtered back-projection algorithm. Figure 4(a) is the picture of the blood vessels in the rabbit ear; (b), (c), and (d) are the reconstructed PA images of the marked areas A, B, and C shown in Fig. 4(a) respectively, which are obtained by means of the limited-field-filtered back-projection algorithm. Clearly, Figs. 4(b)–4(d) show that positions and structures of the targets in the reconstructed image are consistent with the real sample. The reconstructed PA images have very high soft-tissue contrast, though the collected PA signals are not accumulatively averaged.

Due to the limitation of small beam size restricted by the laser pulse energy, only part of the blood vessels can be imaged at present. If a laser system with high pulse energy and large beam size is used, PA image of a large area of blood vessels or tissue can be obtained at a high speed with MLTAS. By using optical contrast agents (for example, indocyanine green) and choosing appropriate laser light as the excitation source, combining MLTAS with molecular probe techniques, the identity molecules or the targeted tissues tagged with molecular probes are selectively excited by a tunable-wavelength laser. The photoacoustic signals will be greatly amplified, and the contrast of the PA image can observably be improved. So, fast photoacoustic molecular imaging based on the multielement phase-control will be made by using this system. These are our next works.

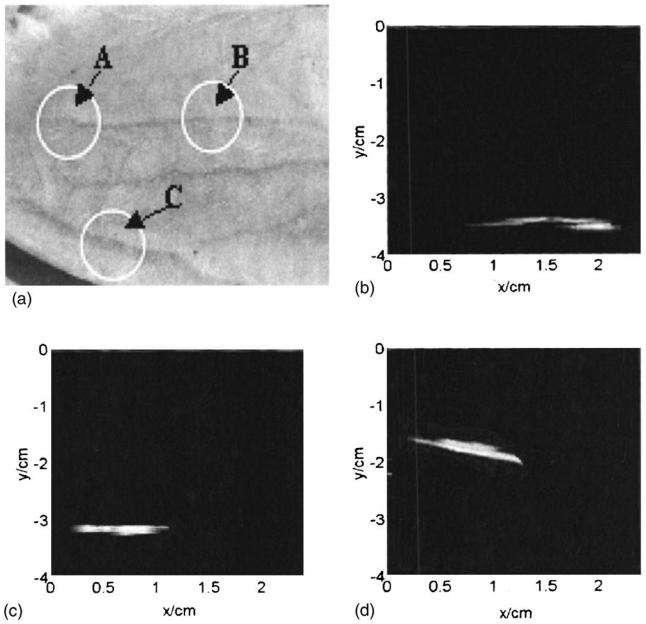

FIG. 4. Photoacoustic reconstruction of parts of *in vivo* blood vessels of a rabbit ear. (a) The picture of the rabbit ear; (b), (c), and (d) are the reconstructed PA images of the marked areas A, B, and C shown in (a), respectively, which are obtained by means of the limited-field filtered back projection algorithm.

In conclusion, we have demonstrated two-dimensional fast photoacoustic imaging with the multielement phase-controlled technique and the limited-field-filtered back-projection algorithm. By taking advantage of less time for data acquisition, satisfactory spatial resolution and good soft-tissue contrast, the methodology and the MLTAS can provide a fast and reliable approach for *in vivo* noninvasive imaging and clinic diagnosis.

This research is supported by the National Major Fundamental Research Project of China (30470494), the National Natural Science Foundation of China (60378043) and the Research-Team Project of the Natural Science foundation of the Guangdong Province (015012).

[1]Roy. G. M. Kollkman and John. H. G. M. Klaessens, Phys. Med. Biol. **49**, 4745 (2004).
[2]R. A. Kruger, W. L. Kiser, D. R. Reinecke, G. A. Kruger, and K. D. Miller, Molecular Imaging **2**, 113 (2003).
[3]J. J. Niederhauser, M. Jaeger, and M. Frenz C., Proc. SPIE **4960**, 118 (2003).
[4]A. A. Oraevsky, E. V. Savateeva, S. V. Solomatin, A. A. Karabutov, V. G. Andreev, and Z. Gatalica, Proc. SPIE **4618**, 81 (2002).
[5]X. D. Wang, Y. J. Pang, G. Ku, G. Stoica, and L. V. Wang, Opt. Lett. **28**, 1739 (2003).
[6]T. O. McBride, B. W. Pogue, S. Jiang, U. L. Osterberg, and K. D. Paulsen, Opt. Lett. **26**, 822 (2001).
[7]R. A. Kruger, P. Liu, Y. R. Fang, and C. R. Appledorn, Med. Phys. **22**, 1605 (1995).
[8]K. P. Köstli and P. C. Beard, Appl. Opt. **42**, 1899 (2003).
[9]X. Wang, Y. Xu, M. Xu, S. Yokoo, E. S. Fry, and L. V. Wang, Med. Phys. **29**, 2799 (2002).
[10]Yi Wang, Da Xing, Yaguang Zeng, and Qun Chen, Phys. Med. Biol. **49**, 3117 (2004).
[11]G. Paltauf, J. A. Viator, and S. A. Prahl, Proc. SPIE **4256**, 138 (2001).
[12]J. J. Niederhauser, M. Jaeger, and M. Frenz, Appl. Phys. Lett. **85**, 2983 (2004).
[13]Yin Bangzheng, Da Xing, Yi Wang, Yaguang Zeng, Yi Tan, and Qun Chen, Phys. Med. Biol. **49**, 1339 (2004).
[14]Yaguang Zeng, Da Xing, Yi Wang, Bangzhen Yin, and Qun Chen, Opt. Lett. **29**, 1760 (2004).